



### **Science Arts & Métiers (SAM)**

is an open access repository that collects the work of Arts et Métiers Institute of Technology researchers and makes it freely available over the web where possible.

This is an author-deposited version published in: <https://sam.ensam.eu>  
Handle ID: <http://hdl.handle.net/10985/7419>

#### **To cite this version :**

Rémy MARCHAL, Frédéric MOTHE, Bernard THIBAUT, Laurent BLERON, Louis DENAUD - Cutting Forces in basic and real life wood machining processes review, COST Action E35 2004-2008: Wood machining - Micromechanics and fracture - Holzforschung - Vol. 63, n°2, p.157-167 - 2009

Any correspondence concerning this service should be sent to the repository

Administrator : [scienceouverte@ensam.eu](mailto:scienceouverte@ensam.eu)



1 **CUTTING FORCES IN BASIC AND REAL LIFE WOOD MACHINING PROCESSES**  
2 **Review Paper**

3  
4 Rémy MARCHAL <sup>\*,1</sup>, Frédéric MOTHE <sup>2</sup>, Louis-Etienne DENAUD <sup>3</sup>,  
5 Bernard THIBAUT <sup>4</sup>, Laurent BLERON <sup>1</sup>

6  
7 <sup>1</sup> Arts et Métiers ParisTech, LABOMAP,  
8 rue Porte de Paris, 71250 Cluny, France [remy.marchal@cluny.ensam.fr](mailto:remy.marchal@cluny.ensam.fr)

9  
10 <sup>2</sup> INRA, LERFOB, Champenoux, 54280 Seichamps, France

11  
12 <sup>3</sup> Université Paul Sabatier, LGMT-, 1 rue Lautréamont, 65016 Tarbes cedex, France

13  
14 <sup>4</sup> CNRS, EcoFoG, BP 709, 97379 Kourou Cedex, France

15  
16 **Abstract**

17  
18 The data available in the literature concerning wood cutting forces permit to build models or  
19 to simulate the main wood machining processes (milling, sawing, peeling etc.). This approach  
20 contributes to a better understanding of formation of wood surfaces and chips and the data  
21 may be helpful to optimize cutting geometry, reduce tool wear, improve tool material, and to  
22 size tool-machines.

23 The models may also be useful for industrial application in two ways: (1) providing  
24 data to optimise the settings for a given operation (batch approach) and (2) building predictive  
25 models that could be the basis of an online control systems for the machining processes  
26 (interactive approach). A prerequisite for this is that numerous machining tests on different  
27 wood materials are performed based on experiences with different kind of tools and  
28 experimental devices. With potential industrial applications in focus, the emphasis of this  
29 review was on the wood peeling process, which is a very demanding special case of wood  
30 cutting. Though not so many industrial machines are equipped with expensive force sensors,  
31 there is a lot of high quality information available about cutting forces which may be useful to  
32 improve the scientific or technologic knowledge in wood machining. Alternative parameters,  
33 such as vibration or sound measurements, appear to be promising substitutes in the praxis,  
34 particularly to feed online control systems of any wood cutting process.

35 **Keywords**

36 cutting forces; online control; peeling process; physico-mechanical model; sound; vibrations;  
37 wood industry; wood machining

38

39

40 **Introduction**

41 *Why to measure cutting forces?*

42 In the course of cutting process analysis, very often cutting forces are chosen as the main  
43 output for physical description of the process. The other possibilities – like vibration, sound,  
44 temperature, cutting power, deformation, surface quality and chip quality measurements – are  
45 usually neglected. The main reason: measurement of cutting force is a powerful tool allowing  
46 to build physico-mechanical cutting models for a better understanding of the phenomena  
47 observed during cutting. These models permit to design or optimise processes, machines,  
48 tools and wood preparation.

49 Cutting models have been first developed on scientific basis in order to describe the  
50 formation and typology of chips related to given cutting forces levels (Kivimaa 1950; Franz  
51 1958). The model of Merchant (1945), written for orthogonal cutting of metal, was adapted to  
52 wood by McKenzie (1960).

53 Other models aiming at the analysis of the wood-tool interaction during machining,  
54 were focusing more particularly on the influence of the cutting geometry (clearance and rake  
55 angles), wood characteristics (species, density, moisture content, and temperature), and  
56 processing parameters (cutting speed, depth of cut) on the level and stability of cutting forces  
57 (Kivimaa 1950; McKenzie 1960).

58 Some authors preferred a mechanical approach based on the cutting forces and  
59 evaluated the stress fields induced by the cutting process into the wood and into the tool,  
60 considering the friction on the surface between the wood and tool. The resultant cutting forces  
61 were divided into two categories: (1) forces exerted by the rake face and (2) forces exerted by

62 the clearance face of the tool (Thibaut 1988). When introducing the tool deflection (Decès-  
63 Petit 1996), the assessment of the cutting plan displacements became possible.

64 Some models have been elaborated to predict cutting forces, to understand the  
65 mechanical behaviour of the materials tested (McKenzie 1962; Eyma et al. 2004) and other to  
66 characterise the machinability of different wood materials (see Kivimaa et al. as quoted by  
67 Scholtz and Troeger 2005). Another important target of these models was a diminishing  
68 expensive experimentation efforts under consideration of all parameters of processing and  
69 materials.

70 Cutting forces have been frequently measured to size motors for machine tools to  
71 decrease energy consumption and to optimise processing parameters – such as cutting speed  
72 (Liska 1950; Sinn et al. 2005) –, depth of cut (Axelsson et al.1993), feed rate (Ko et al. 1999)  
73 and upward/downward milling (Palmqvist 2003; Goli et al. 2003). The cutting forces have  
74 also been used to optimise the tool geometry, e.g. rake, wedge and clearance angles, tool edge  
75 direction (Woodson and Koch 1970; McKenzie and Karpovich 1975; Komatsu 1976; Stewart  
76 1977; Komatsu 1993; Boucher et al. 2004), and the tool head design (e.g. the chip space,  
77 Heisel et al. 2004; Heisel et al. 2007).

78 Cutting forces have often been measured to compare the cutting properties of different  
79 tool materials, e.g. steel, carbide, diamonds, thermal treated tools, and coated tools (Stewart  
80 1991; Darmawan et al. 2008). Also the machined wood was in focus considering the grain  
81 orientation and the structure (Axelsson 1994; Cyra and Tanaka 1999; Goli et al.2003), the  
82 heterogeneity (Mothe 1988), the moisture content (Kivimaa 1950), the temperature of  
83 steamed or frozen wood (Marchal et al. 1993, Lundberg and Axelsson 1993), the mature or  
84 the juvenile wood (Gonçalves and Néri 2005), the tension or the normal wood (Vazquez-Cooz  
85 and Meyer 2006), and the type of wood based materials. In the latter case, often modified  
86 MDF (Kowaluk et al.2004) or not modified MDF (Ko et al. 1999) was investigated.

87           The avoidance of dust and noise, and the improvement of the productivity (reduction  
88 the tool changing time, increase of the cutting speed, of the feed rate and of the cutting depth  
89 for a given surface quality) were also frequently in focus. Important results were obtained  
90 with this regards concerning predicting the tool edge wear (Fischer 1999; Fischer 2004),  
91 online controlling the wear (Huang, Y.-S 1994; Cyra and Tanaka 1999), predicting the chip  
92 geometry and fragmentation (Franz 1958), and online monitoring the wood surface quality  
93 (Cyra and Tanaka 1999; Palmqvist and Johansson 1999; McKenzie et al. 2001).

94           In some specific cases, the measurements of cutting forces helped to quantify the  
95 efficiency of auxiliary devices used to assist the cutting processes – e.g. ultrasonic-assisted  
96 cutting (Sinn et al. 2004) – or to improve the use of a pressure bar (Mothe and Marchal 2001).

#### 97 *How to measure cutting forces?*

98 Two main approaches are known to measure cutting forces.

99 (1) Direct measurements by sensors directly placed on the tool or in strategic points on the  
100 frame. Strain gauges and piezo electric sensors are common. Strain gauges technology is  
101 cheap but not always efficient. Dynamometers, specifically designed for measuring cutting  
102 forces of wood, have some drawbacks especially for trials involving very small forces, which  
103 is quite often the case in wood machining. Sometimes, the ground noise and the signal cannot  
104 be differentiated. Such devices need a very meticulous set-up including an important  
105 management of wiring. Nevertheless, they are highly sensitivity to temperature and moisture.  
106 Another limiting factor is their low stiffness because they are based on deformation  
107 measurements. Piezo electric sensors are more expensive and much stiffer. They are reliable  
108 on several decades of forces values, are easy to maintain, and, – despite a drift of about 0.01  
109 N/s in case of static test – are well adapted for dynamic and semi-static mechanical  
110 measurements.

111 (2) Indirect measurement are also available, which are based on non-contact displacement  
112 sensors with eddy current technology to measure distances, displacements. The forces are  
113 then computed via an inverse function of transfer (Costes 2007).

114 ***Which cutting force components to consider?***

115 When measuring cutting forces, for the case of orthogonal cutting, the resultant force is  
116 usually decomposed in two ways: (1) in two orthogonal components: parallel and normal  
117 forces (Figure 1) and (2) in two facial components: rake and clearance forces (Figure 2).

118 The first decomposition seems often suitable from the technological point of view.  
119 The parallel force gives information on the torque and consequently the energy consumption.  
120 The normal force describes the plunging or cutting refusal tendency as well as the tool wear  
121 (Palmqvist 2003). The thickness of the damaged layer arisen during planing is also described  
122 (Hernandez and Rojas 2002). Force variations are linked up with the roughness of the wood  
123 surface.

124 The second decomposition makes it possible to propose a model directly linking the  
125 facial component forces to mechanical characteristics of wood. Such a model is much more  
126 powerful than the first one for the physical understanding of the underlying phenomenon, and  
127 at the same time, it is of some interest for optimising cutting geometry. On the other hand,  
128 two main hypotheses are necessary to use such a facial decomposition: (1) The sharpness of  
129 the tool is very good, i.e. the radius of the tool tip is low enough to neglect the “front” forces  
130 on the tool tip compared to the two facial components. (2) There is only Coulomb friction  
131 between tool and wood.

132 Franz (1958) and Kivimaa (1950) and many other authors favoured obviously the first  
133 approach. Few authors adopted the second way: Dippon et al. (1999) for orthogonal cutting of  
134 MDF, Thibaut (1988) and Thibaut and Beauchêne (2004) for the study of 0/90° cutting mode  
135 on green wood (peeling or slicing). Fischer (2004) mixed the two approaches in order to

136 describe the phenomena at the mesoscopic scale just behind the cutting edge and, considering  
137 the forces under and above the cutting line. This author proposed a global approach of wood  
138 machining with specific trajectories of the tools into wood materials when milling, sawing or  
139 drilling.

#### 140 *From the basic to the industrial praxis*

141 Measurement of cutting forces during wood machining is nowadays easy to realise at  
142 laboratory scale and physical models of cutting can be constructed which are capable of  
143 simulating the process. Different authors developed specific devices. These are necessary: (1)  
144 In the case of a **batch processing** for the prediction of machinability of some given wood  
145 materials and/or setting-up of specific machining operation. (2) In the case of an **interactive**  
146 **processing** to build a predictive model, then a monitoring system based on measurement of  
147 forces. These can be applied to adjust online process parameters (the cutting speed and/or the  
148 cutting geometry) based either on an open loop (help to the decision system for operators) or  
149 on a closed loop (adaptive control) control.

150 Nevertheless, in this last case, cutting forces do not always appear to be the most  
151 suitable inputs because of the specific and very expensive design of the machine-tools.  
152 Moreover, the integration of gauges in the internal structure of a device often reduces a  
153 machine's rigidity. Substitute outputs for control purposes must then be found.

154 To illustrate all these aspects, this paper is focused on the peeling process because it is  
155 an industrial process following a fundamental cutting mode ( $0^\circ/90^\circ$ ). A direct transfer of the  
156 results from the laboratory scale to the industrial one is possible.

157 The peeling process requires keeping very accurate settings all along the machining  
158 operation. Actually, the cutting forces being the lowest among all wood processes (mode  
159  $0^\circ/90^\circ$ , green wood), the tool balance is very sensitive to any change – even minor – of  
160 settings and of wood properties. Critical cutting plan displacements easily occur inducing

161 veneer thickness variation because of the high transverse deformability of green and often  
162 heated wood blocks stressed by the knife. Moreover, the action of the pressure bar modifies  
163 forces equilibrium and its settings interlink with the knife's settings. In peeling process the  
164 final product (the veneer) being the chip, a carefully setting of all parameters is very  
165 important in order to obtain both a good quality chip and machined surface, but also to reach  
166 as fast as possible the steady state and to keep it.

## 167 **Model of cutting forces to simulate the process**

### 168 *Mechanics of peeling process*

169 Thibaut (1988) and Thibaut (1995) proposed a system of mechanistic models for describing  
170 the basic processes in rotary veneer cutting. The experimental analyses were performed by a  
171 microlathe (Figure 3). This device permitted to record cutting forces and to visualise the  
172 lateral section of the piece of wood during the process (Butaud et al. 1995). The models of  
173 Thibaut explained and reproduced most of the experimental observations resulting from  
174 numerous peeling trials of various species like chestnut (Movassaghi 1985; Thibaut 1988),  
175 Douglas-fir (Movassaghi 1985; Mothe 1988), oaks (Marchal 1989), beech, walnut and poplar  
176 (Deces-Petit 1996), numerous tropical woods (Thibaut 1988; Beauchêne 1996).

177 The main experimental observations may be summarised as follows after the analysis of  
178 the forces exerted by the tool (the resultant rake force  $F_a$ , the resultant clearance force  $F_d$ ) and  
179 by the pressure bar ( $F_b$ ), and also considering their respective tangential (or parallel) and  
180 radial (or normal) components X and Y (Figure 2):

181 The chip flows above the rake face of the tool via a shearing deformation along a nearly  
182 radial plane (zone 2 in Figure 4), and does not show any shortening as compared to cutting  
183 length, which is in strong disagreement with classical metal machining experiments and  
184 theories like that of Merchant.



185           The compression and rubbing action of the pressure bar – most of the experiments were  
186 performed with a nosebar; the action of a round bar would be slightly different – and the  
187 clearance face of the tool result in radial compressive stresses which can reach very high  
188 values (crushing of the cells – zones 1 in Figure 4) near the contact zone, and remain in the  
189 elastic domain farther from the tool (zone 4 in Figure 4).

190           The radial wood displacement at the tip level leads to unexpected changes of the final  
191 thickness of the veneer due to this compression state (Figure 5).

192           In front of the tool tip, the radial tensile stresses resulting from both tool and bar actions  
193 may lead to lathe checks (in mode I), particularly for thick veneer and dense wood (zones 3 in  
194 Figure 4, Figure 6a).

195           For lower thickness and softer wood, the tangential compression at the tool edge level  
196 may lead to discontinuous cutting with alternation of wood compression and relaxation in  
197 front of the tool tip. This behaviour is often called the Horner effect (Figure 6b).

#### 198 *Simulation of the peeling process*

199           The models of Thibaut were embedded into a software for simulating the rotary cutting of a  
200 heterogeneous wood (Mothe et al.1997). The simulation works on a radial basis: starting from  
201 the initial conditions (tool edge tangential to the surface, veneer thickness = 0), the cutting  
202 forces are computed for each rotation at the same angular position (Figure 7), as the tool  
203 moves radially inwards. The radial wood displacement induced by the cutting forces is  
204 therefore computed, allowing predicting the actual veneer thickness at each turn.

205           It was assumed that wood properties remain constant – at least in a short distance – in  
206 both tangential and longitudinal directions and vary only along the radius. Beauchêne and  
207 Thibaut (1996) showed that most of the mechanical properties of wet wood depend strongly  
208 on the wood density and temperature for tropical homogeneous species. The stress-strain  
209 curves in radial compression, in radial tension, and in radial/tangential shear are all supposed

210 to be predictable at a given temperature through the wood density profile from the tip of the  
211 pressure bar to the inner core.

### 212 ***Force on the pressure bar ( $F_b$ )***

213 The radial component of  $F_b$ ,  $Y_b$ , is related to the depth of wood crushed by the pressure bar  
214 which is the difference between the actual veneer thickness  $E_v$  and the horizontal gap  $Ch$ . The  
215 radial displacement is absorbed by the whole block of wood from the upper side of the veneer  
216 to the peeling lathe spindle (not considering the bolt bending).

217 The radial force may be computed with an iterative procedure: For increasing values  
218 of the load, the stress distribution is estimated along a plane uniformly loaded with the  
219 formula of Timoshenko and Goodier (1951). The radial displacements of elementary portions  
220 of wood are summed along the radius to compute the total wood displacement: The process is  
221 repeated until the total displacement is close enough to the bar penetration  $E_v - Ch$ .

222 Finally, an experimental model based on the pressure bar settings and the friction  
223 coefficient is applied for estimating the orientation angle of  $F_b$  and therefore the tangential  
224 component  $X_b$ . Assuming that the compression load is identical on both the front and back  
225 faces of the pressure bar, the total force is redistributed on both faces proportionally to the  
226 respective lengths of contact, which are computed geometrically.

### 227 ***Force on the tool clearance face ( $F_d$ )***

228 The clearance force  $F_d$  depends mainly on the amount and stiffness of wood crushed by the  
229 clearance face. The depth and length of contact are computed geometrically based on the  
230 actual veneer thickness, the peeling radius, and the clearance angle. The radial component is  
231 then calculated by the same iterative procedure as for the pressure bar force.

232 However, experimental results show that  $F_d$  remains rather high even if the clearance  
233 angle is large enough to minimise the contact. This can be explained by the crushing of cells  
234 rolling back the tool edge and rubbing the clearance face on a short distance. This second

235 contribution to the radial component of  $F_d$  can be estimated by the product of the contact  
236 length (supposed to be constant) and the stress generated by the cells crushing (supposed to be  
237 equal to the end of the elastic phase of the stress-strain curve in radial compression).

238 With the radial component of the clearance force being known, the angle of inclination  
239 of  $F_d$  (given by the friction coefficient between wet wood and metal) can be used to compute  
240 the tangential component of the clearance force.

#### 241 ***Force on the tool rake face ( $F_a$ )***

242 The rake force  $F_a$  increases quite linearly with wood density and veneer thickness. It depends  
243 mainly on the intensity of the stresses and their distribution along the main shearing plane.

244 **In absence of a pressure bar**, the radial force may be estimated by integrating along  
245 the stresses along the shear plane (supposedly radial). Considering that the wedge angle is  
246 usually close to  $20^\circ$ , the maximal shear deformation near the tool tip may be assumed to be  
247 constant (around 35%) whatever the lathe settings are. An exponential decreasing function is  
248 then used to describe the stress distribution and to compute the radial component of  $F_a$ .

249 **In the presence of a pressure bar**, the forces on both the back and front faces of the  
250 bar have to be considered. The radial component of the back face force contributes positively  
251 to the rake force, the veneer being compressed between the back face of the bar and the rake  
252 face of the tool (this force is null if the angle between the cutting plan and the back face is  
253 above  $90^\circ$ ). On the other hand, the front face force contributes negatively by reducing the  
254 stresses along the shearing plane.

#### 255 ***Radial wood displacements due to the cutting forces***

256 The radial forces on the tool and the pressure bar lead to radial displacement of the wood  
257 block. As a main consequence, the veneer thickness ( $E_v$ ) may be slightly different from the  
258 expected thickness.

259           The actual thickness depends on the current radial displacement and on the  
260 displacement resulted from the previous revolution. Assuming that the previous displacement  
261 and the cutting forces are known, the new displacements generated at the tool tip level by the  
262 radial components of the shearing force, the tool clearance force and the front face of the  
263 pressure bar force have to be computed. The force on the back face of the nosebar is assumed  
264 have no effect because it is equilibrated by the face force of the tool rake. In each case, this  
265 task is performed by summing along the radius the displacements of elementary layers of  
266 wood in accordance with the relationships between tension and compression stress-strain.

### 267 *Main calculation loop*

268           Considering that the cutting forces are needed for estimating the veneer thickness and that the  
269 thickness depends on the cutting forces, an iterative procedure has to be applied. The  
270 convergence is usually reached after less than five iterations for heterogeneous woods except  
271 when the properties change abruptly (e.g. near an annual ring limit) or when the pressure bar  
272 (being misplaced) leads the tool to plunge and rise alternately.

### 273 *Veneer quality*

274           The three main defects of a rotary cut veneer linked to the cutting process are lathe checks,  
275 roughness due to the Horner effect, and thickness variations. Only the last one has been  
276 actually predicted by the simulator, even if lathe checks and Horner effect could be predicted  
277 easily through cutting forces and tensile properties of wood.

278           For heterogeneous wood species, the continuous changes in wood density tend to  
279 make worse these defects. The most unfavourable case occurs when the wood density near the  
280 pressure bar and near the tool are strongly different, as shown for the two main cases in figure  
281 6 frequently occurring when peeling softwoods.

282           A virtual simulation of the peeling process is nowadays available to predict cutting  
283 forces, and consequently the adapted settings for given wood species. However, this model

284 can be improved with better modelling of wet wood mechanical behaviour. With a view to  
285 deliver a more general model of the chip formation during peeling at the mesoscopic scale,  
286 Bonin (2006) attempted to implement a thermo-mechanical simulation of metal turning  
287 (Cordebois 1994; Ali, F. 2001) to wood peeling. An adaptation of the thermo mechanic model  
288 of Oxley (1989) has been tested based on a law of wood orthotropy (called the Bauschinger  
289 effect; asymmetry of the mechanical behaviour in compression and tension) and considering  
290 the deformation speed. This approach was unsuccessful because all the analytical models of  
291 the chip formation for metals are based on laws describing elastoplastic behaviour at high  
292 deformations. After having performed a great number of mechanical tests on beech green  
293 wood in transverse directions, Bonin (2006) concluded that hyperelasticity and  
294 compressibility of green wood like elastomers (Laraba-Abbes 1998) caused the differences.  
295 Bonin (2006) also built a new model relying on simplified assumptions (e.g. neglecting the  
296 increase of temperature during chip formation and the orthotropy in the transverse plan) based  
297 on thirty micropeeling tests. In this model, the slope of the cutting zone was in agreement  
298 with the experiments. Furthermore, forces occurring on the rake face of the tool were  
299 correctly predicted: for more than 95% of the predicted forces, the gap between experimented  
300 and predicted results was less than 20%.

### 301 **Dynamometric approach for optimising the process**

302 From this comprehensive description of the veneering process, several practical rules can be  
303 highlighted which are directly applicable to industrial processes. Just considering the two  
304 decompositions of  $F_c$ , the resultant cutting force exerted by the tool, the 4 components provide  
305 useful practical information on the process in progress:

306 (1)  $X_c$ : its mean value determines the lathe motor torque value. It must be as small as  
307 possible. Standard variation of  $X_c$  is linked to the amplitude and possibly the frequency of  
308 lathe checking.

309 (2)  $Y_c$  is linked to the tool tip position: a negative value expresses a cutting refusal  
310 tendency when a positive one indicates a tool plunging tendency. In the normal case, the best  
311 settings are obtained when the tool dives a little (low positive  $Y_c$  value); the cutting plan is  
312 then slightly lower than the theoretical one. As can be seen in Figure 8, a very small change  
313 on clearance angle can then induce huge effect upon the tool equilibrium, especially for very  
314 small veneer thicknesses (Marchal and Negri 1997).

315 (3) The ratio  $F_a/F_d$  describes the tool balance and also the wear pattern. In the normal  
316 case,  $F_a/F_d$  is in the range of 2 to 3.  $F_a$  and  $F_d$ , are computed as illustrated in Figure 2. These  
317 two forces are, respectively, a function of the veneer thickness and of the clearance angle. It is  
318 quite easy to act on the clearance angle to reach the right ratio. This ratio must be as  
319 insensitive as possible to cutting speed variation. There are for a given wood species two  
320 domains: one for low cutting speed and one for high cutting speed. At high speed, the  
321 clearance angle should be increased in order to avoid the huge increase of  $F_d$  (Figure 9 in the  
322 case of walnut) due to the “Maxwell effect” and then to maintain the good balance of the tool.  
323 Cutting speed and clearance angle are interlinked settings. Remark to the Maxwell effect:  
324 Under high deformation speeds, free water contained in cells being only partly evacuated  
325 from the maximum stress area, the free water still remaining induces an apparent increase in  
326 rigidity through Young’s modulus because of its incompressibility (Costes and Larricq 2002).

327 (4) All the mean values and the variation of forces must be maintained at a level as low as  
328 possible in order to improve tool-life (minimizing the wear of the tool and machine fatigue).

329 Considering also the pressure bar, (1) The ratio  $Y_b/F_a$  can be used to survey the pressure  
330 bar efficiency for reducing lathe checking (Thibaut 1988). (2) The sum  $X_c+X_b$  should be  
331 minimized to decrease the power consumption and (3) the sum  $Y_c + Y_b$  should be minimized  
332 to decrease the flexion of the wood block at the end of the process.

333           These measurements and calculation are very useful for the process optimisation at the  
334 laboratory scale. However, there are not yet industrial machines equipped with force sensors  
335 which make possible the application of this knowledge neither for basic optimisation nor for  
336 online control of the process (Lemaster et al.2000a). Nevertheless, for high value added  
337 products, the process could be feasible.

## 338 **Cutting forces and alternative outputs to develop interactive processing**

### 339 *Power consumption*

340 Some alternative inputs were also investigated. The nearest measurement to forces is probably  
341 power consumption. Despite the fact that it is quite easy to implement directly a spindle to  
342 measure the power consumed by the cut, this information is significantly less pertinent.  
343 According to Lemaster et al. (2000a), this measurement integrates both the cutting forces and  
344 the dynamic aspects of the machine.

### 345 *Artificial vision*

346 Operators on CNC often characterise the status of the process by visual inspection. Many  
347 defects of the machined surface or tool wear can be seen directly. Unfortunately, according to  
348 Januten (2002), direct methods to measure tool wear (also including computer vision) have  
349 not yet proven to be very attractive economically and technically. Lemaster and Stewart  
350 (2005) have developed a software able to distinguish different random defects from an optical  
351 profilometer signal. The algorithm proposed is based on fuzzy logic and Wavelets. This  
352 approach seems very promising, but it is still not yet fully developed.

### 353 *Acoustic emission*

354 Several authors also applied acoustic emission (AE) as input data. AE is the stress waves (low  
355 energy and very high frequency i.e. from 100 kHz up to 1000 kHz) produced by the sudden  
356 internal stress redistribution of a material caused by changes in its internal structure (crack  
357 opening or growing, fibre breakage, etc.). Lemaster et al. (1982), Lemaster and Kato (1991),

358 and Murase et al. (2004) proved the great potential of this technique to monitor wood cutting  
359 processes. According to the accepted indicators (Root Mean Square - RMS, count rate,  
360 cumulative count rate, etc.), AE is sensitive to the chip formation mechanism (shearing plan,  
361 sliding areas, cracks, splits etc.). However, Lemaster et al. (2000a) underlined the limitation  
362 of this technique which is the high sensitivity to background noise due to the device  
363 components such as roller bearings. Adding the high damping character of wood materials, it  
364 is necessary to place sensors very closed to the cutting area, which is often not applicable in  
365 industry.

### 366 *Sound and vibrations*

367 Experienced operators are very sensitive to sound or vibrations emitted by the process of  
368 milling or sawing (Marchal et al. 2000). Only a few works were carried out with acoustic or  
369 vibratory sensors as sources of information for wood machining. Nagatomi et al. (1999) found  
370 a high correlation between probability of sound pressure level (SPL) larger than a suitable  
371 threshold and surface roughness of peeled veneers of sugi. However, this relation was  
372 obtained within a very large domain of frequencies (some Hz to 100 kHz) which is not  
373 congruent with the operator's ability with an audible range from 20 Hz to 20 kHz. In  
374 numerous other works based on AE or SPL measurements to build an online control system  
375 (Tanaka et al. 1997; Nagatomi et al.1993; Murase and Harada 1995), the threshold value  
376 determination has never been clearly explained. This value is always more or less linked to  
377 experimental settings applied (device, wood species, cutting conditions, moisture content,  
378 etc.) which is not enough flexible to meet industrial requirements. Iskra and Tanaka (2006)  
379 used dynamical thresholds to analyse (one-third octave band analysis) both SPL and sound  
380 intensity during routing of Japanese beech. This constituted a great improvement of the  
381 approach previously described because the criterion was polyvalent and consequently better  
382 adapted to industrial environment constraint.



383 Iskra and Tanaka (2005) obtained a significant and high correlation coefficient  
384 between surface roughness and sound intensity allowing them to adapt feed rate during  
385 routing with regard to the value of sample grain angle. However, the frequency band selected  
386 for computation was probably only optimal for the experimental setup considered. Lemaster  
387 et al. (2000b) used accelerometers and obtained similar results for tool wear monitoring  
388 during routing. Instead of a global RMS value (computed on a large frequencies domain), the  
389 authors proposed power spectrum density (PSD) as criterion to determine the most promising  
390 band for computation. The great potential of spectral analysis was confirmed by Denaud et al.  
391 (2005). During peeling, the authors identified a peak on fast Fourier transform (FFT) spectra  
392 (obtained from both microphone and accelerometers as indicated in Figure 10). It corresponds  
393 to the vibratory signature of the average lathe check frequency of the veneer. This  
394 phenomenon is almost periodic for homogeneous species. However, the peak detection would  
395 be only possible by characterising the mechanical behaviour of the lathe which is a delicate  
396 and an expensive operation. To bypass this difficulty, Denaud et al. (2007a) developed a  
397 method to identify the signature of lathe checks on the temporal signal emitted from the same  
398 sensors. This needs only a local RMS averaging via a peak detection algorithm which did not  
399 require any threshold (see Figure 11). This approach seemed very promising to get check  
400 distributions along the veneer, however, its efficiency for slightly checked veneers was not  
401 characterised.

402 To sum up, vibration or sound measurements seem to be the most promising ways to  
403 substitute measurements of cutting forces in a search for an online control system of a cutting  
404 process. However, there are some ambiguities concerning a threshold, a correlation  
405 coefficient, a frequency band domain or a peak on a spectral analysis. Hitherto, empirical and  
406 preliminary limits are set with this regard.

407 As a response, Denaud et al. (2007b) initiated new experiments. These authors tried to  
408 avoid any check formation and estimated PSD from a “reference cutting trail” under  
409 conditions of a high pressure rate of the pressure bar (20% of the veneer thickness here). In  
410 this manner, they took account of the dynamical behaviour of their device. Such settings  
411 produced inevitably unacceptable variations of the veneer thickness which, however, did not  
412 affect notably the PSD.

413 The ratio between measured and reference signal helped avoid natural frequencies of  
414 the lathe. By this way, the default signature characterisation was greatly simplified as shown  
415 in Figure 12 for the same domain of frequencies. The highest peak was at 152 Hz which  
416 corresponds to an average distance of almost 3.3 mm between two consecutive checks.  
417 Moreover, according to the results of Denaud et al. (2007b), this approach is also suitable for  
418 relatively low pressure rates. In the end, this could lead to an online control of the pressure  
419 rate of the pressure bar which is always a compromise to obtain a veneer with small lathe  
420 checks and constant thickness.

## 421 **Conclusion**

422 For a long time, cutting force measurement has been the only successful and most powerful  
423 measurement for producing output data for advanced analytical research on wood machining  
424 processes. It is still matchless and helps improve knowledge about wood surface formation  
425 and tool wear. Its main asset is that it takes into consideration the contact between tool and  
426 wood and thus enables computation of the strains inside the wood pieces, the wood chips, and  
427 the tools. However, cheaper sensors with more operating comfort are needed in the industrial  
428 praxis. Against this background, accelerometers and microphones, which can be integrated  
429 easily into the machine, are promising sensors for the near future. On the other hand, the  
430 signal treatment is more difficult in the case of these sensors.

431 Measuring wood cutting forces makes a sense definitively for basic research. The  
432 same is true in industrial applications, particularly in batch processes. In such cases,  
433 preliminary tests on specific machining benches are necessary in order to optimise cutting  
434 geometry and any other cutting parameters, before launching a new production.

#### 435 **References**

436 Ali, F. (2001) Modélisation et simulation thermomécanique de la coupe des métaux. ENSAM  
437 PhD thesis, Paris, 284 p.

438 Axelsson, B.O.M. (1994) Lateral cutting force during machining of wood due to momentary  
439 disturbances in the wood structure and degree of wear of the cutting tool. Holz Roh Werkst 52  
440 (3): 198 - 204

441 Axelsson, B.O.M., Grundberg, S.A., Grönlund, J.A. (1993) Tool wear when planning and  
442 milling. Measurement methodology and influencing factors. Proceeding of IWMS 11, May,  
443 25-27 1993, 159-176

444 Beauchêne, J. (1996) Evolution du comportement mécanique du bois vert avec la  
445 température. Application à l'étude du déroulage et du tranchage de quelques bois guyanais.  
446 ENGREF PhD thesis, Montpellier, April 1996, 164 p+ann.

447 Beauchêne, J., Thibaut B. (1996) Influence de la température sur le comportement mécanique  
448 du bois vert : application à l'étuvage d'essences guyanaises en vue du déroulage. Proceedings  
449 of "Quatrième Colloque Sciences et Industries du Bois", Nancy, 11-13 septembre 1996,  
450 p 299-306.

451 Bonin, V. (2006) Modélisation analytique de la déformation du copeau Durant le procédé de  
452 déroulage de hêtre, Thèse de Mécanique, ENSAM, 273 p.

453 Boucher, J., Méausoone, P.-J., Perrin, L. (2004) Effect of diamond tool edge direction angle  
454 on cutting forces and tool wear during milling of Medium Density Fiberboard and

455 particleboard. Proceedings of the 2<sup>nd</sup> International Symposium on Wood Machining, Vienna  
456 July 5-7, 2004, 399-407

457 Butaud, J.C., Decès-Petit, C., Marchal, R. (1995) An Experimental Device for the Study of  
458 Wood Cutting Mechanisms : the Microlathe. Proceedings of the 12th International Wood  
459 Machining Seminar, October 2-4, 1995, KYOTO (Japan)

460 Cordebois, J.P. (1994) Viscoplastic modelling of cutting in turning, Journal of materials  
461 processing technology, 1994, vol. 41, pp. 187-200

462 Costes, J.-P. (2007) Measurements without contact of vibration during milling : two exemples  
463 of applications in machining operations monitoring. Lecture in Training School of COST  
464 Action E35, Cluny, 5-7 december 2007

465 Costes, J.-P., Larricq P. (2002) Towards high cutting speed in wood milling. Ann. For. Sci. 59  
466 (2002) 857-865

467 Cyra, G., Tanaka, C. (1997) The effects of grain orientation on routing surface, finish, cutting  
468 forces and acoustic emission. Proceeding of IWMS 13, June 17-20, 1997, 323 - 331

469 Darmawan, W, Usuki, H., Quesada, J. Marchal, R. (2008) Clearance wear and normal force  
470 of TiN-coated P30 in cutting hardboards and wood-chip cement boards. Holz Roh Werkst 66:  
471 89-97

472 Decès-Petit C. (1996) Etude des phases transitoires au cours du déroulage de bois. ENSAM  
473 PhD thesis, Cluny, October 1996, 120 p+ann.

474 Denaud, L.-E. (2006) Analyses vibratoires et acoustiques du déroulage. ENSAM PhD thesis,  
475 Cluny, November 2006, 236 p., 2 annexes

476 Denaud, L.E., Bléron, L., Ratle, A., Marchal, R. (2005) Vibro-acoustic analysis of wood  
477 peeling process: temporal and spectral analysis, Proceedings of the 17th IWMS, Sept. 26-  
478 28th, Rosenheim (Germany), pp. 55-65.

479 Denaud, L.E., Bléron, L., Ratle, A., Marchal, R. (2007 a) Online control of wood peeling  
480 process: Acoustical and vibratory measurements of lathe checks frequency. *Ann. For. Sci.*  
481 64:569–575.

482 Denaud, L.E., Bléron, L., Ratle, A., Marchal, R. (2007 b) On-line measurement of the average  
483 lathe checks frequency of peeled veneers. *Proceedings of the 3rd International Symposium on*  
484 *Wood Machining, Lausanne May 21-23, 2007, 77-80.*

485 Dippon, J., Ren, H., Ben Amara, F., Altintas, Y. (1999) Orthogonal cutting mechanics of  
486 Medium Density Fiberboards. *Proceeding of IWMS 14, September 12-19, 1999, 31-40*

487 Eyma, F., Méausoone, P.-J., Martin, P. (2004) Study of the properties of thirteen tropical  
488 wood species to improve the prediction of cutting forces in mode B. *Ann. For. Sci.* 61:55-64

489 Fisher R. (1999) Wood cutting simulation – A program to experiment without a machine.  
490 *Proceeding of IWMS 14, September 12-19, 1999, 553-562*

491 Fisher R. (2004) Microprocesses at cutting edge – Some basics of machining wood.  
492 *Proceedings of the 2<sup>nd</sup> International Symposium on Wood Machining, Vienna July 5-7, 2004,*  
493 191-202

494 Franz, N.C. (1958) *An analysis of the wood-cutting process, Univ. of Michigan Press, Ann.*  
495 *Arbor., Mich., 1958.*

496 Goli, G., Marchal, R., Uzielli, L., Negri, M. (2003) Measuring cutting forces in routing wood  
497 at various grain angles. Study and comparison between u- and down-milling techniques,  
498 processing Douflas-fir and oak. *Proceedings of IWMS 16, Matsue, August 24-30, 2003 127-*  
499 137

500 Gonçalves, R., Néri, A. C (2005) Orthogonal cutting forces in juvenile and mature *Pinus taeda*  
501 wood. *Sci. agric. (Piracicaba, Braz.), vol.62, n°4, Piracicaba July/Aug. 2005, 310-318*

502 Heisel, U., Tröger, J., Martynenko, S. (2004) Aspects on high-performance cutting with  
503 machining centres. Proceedings of the 2<sup>nd</sup> International Symposium on Wood Machining,  
504 Vienna July 5-7, 2004, 161-173

505 Heisel, U., Martynenko, S., Schneider, M. (2007) Influence of chip space filling on cutting  
506 forces in high-speed milling of wood and derived timber products. Proceedings of the 3<sup>rd</sup>  
507 International Symposium on Wood Machining, Lausanne May 21-23, 2007, 51-54

508 Hernández, R.E., Rojas, G. (2002) Effects of knife jointing and wear on the planed surface  
509 quality. of sugar maple wood. Wood Fiber Sci 34:293–305

510 Huang, Y.-S., (1994) Cutting force components in orthogonal cutting parallel to the grain  
511 (90-0). II. Effect of feed lengths. Mokuzai Gakkaishi 40(10): 1059-1066

512 Iskra, P., Tanaka, C. (2005) The influence of wood fiber direction, feed rate, and cutting  
513 width on sound intensity during routing. Holz Roh Werkst 63(3):167-172.

514 Iskra, P., Tanaka, C. (2006) A comparison of selected acoustic signal analysis techniques to  
515 evaluate wood surface roughness produced during routing, Wood Sci. Technol. 63(3):247-  
516 259.

517 Januten, E. (2002) A summary of methods applied to tool condition monitoring in drilling,  
518 International Journal of Machine Tools and Manufacture 42(9):997-1010.

519 Kivimaa, E. (1950) The cutting force in woodworking. Publication number 18. The State  
520 Institute for Technical Research, Finland, Helsinki, 103 p.

521 Ko, P., McKenzie, W., Cvitkovic, R., Robertson, M.F. (1999) Parametric studies in  
522 orthogonal machining MDF. Proceeding of IWMS 14, September 12-19, 1999, 1-12

523 Komatsu, M. (1976), Machine boring properties of wood. II. The effects boring conditions  
524 on the cutting forces and the accuracy of finishing, J. Jap. Wood Res. Soc. 1976 22(9):  
525 491-497.

526 Komatsu, M. (1993) Machining performance of a router bit in the peripheral milling of wood  
527 I. Effects of the radial rake angle of the peripheral cutting-edge on the cutting force and  
528 machined-surface roughness. *Mokuzai Gakkaishi*, 39(6), 628-635

529 Korwaluk, G., Dziurka, D., Beer, P., Sinn, G., Stanzl-Tschegg, S. (2004) Influence of  
530 ammonia on particleboard properties. Proceedings of 2<sup>nd</sup> International symposium on wood  
531 machining, Vienna Austria, 5-7 July 2004, 459-465

532 Laraba-Abbes, F. (1998) Etude des comportements hyperélastiques et viscoélastiques de deux  
533 élastomères de type NR et PDMS par extensométrie optique bidimensionnelle. Thèse  
534 mécanique et matériaux. Paris : Ecole Centrale de Paris, 1998, 295 p.

535 Lemaster, R.L., Klamacki, B.E., Dornfeld, D.A. (1982) Analysis of Acoustic Emission in  
536 Slow Speed Wood Cutting, *Wood Sci.*15(2):150-160.

537 Lemaster, R.L., Kato ,K. (1991) Generation of Acoustic Emission during chip formation, 10th  
538 IWMS, oct., pp. 146-151.

539 Lemaster, R.L., Lu, L., Jackson, S. (2000)(a) The use of process monitoring techniques on a  
540 CNC wood router – Part 1. Sensor selection, *Forest Product Journal* 50(7/8):31-38.

541 Lemaster, R.L., Lu, L., Jackson, S. (2000)(b) The use of process monitoring techniques on a  
542 CNC wood router – Part 2. Use of a vibration accelerometer to monitor tool wear and work  
543 piece quality, *Forest Product Journal*. 50 (9): 59-64.

544 Lemaster, R.L., Stewart, J.S. (2005) Research in Process Monitoring of Surface Quality  
545 Conducted at the North Carolina State University Wood Machining and Tooling Research  
546 Program, Proceedings of the 17th IWMS, Sept. 26-28th, Rosenheim (Germany), pp. 450-467.

547 Liska, J. A. (1950) Effect of rapid loading on the compression and flexural strength of wood.  
548 Forest Products Laboratory Report 1767.

549 Lundberg, A.S., Axelsson, B.O.M. (1993) Studies of the cutting forces and the chip formation  
550 process when cutting frozen wood. Proceeding of IWMS 11, May, 25-27 1993, 57-72

551 McKenzie, W. (1960) Fundamental aspects of wood cutting process. Forest Products Journal,  
552 vol X, n°9, September, 447-456

553 McKenzie, W. (1962) The Relationship Between the Cutting Properties of Wood and  
554 Its Physical and Mechanical Properties. Forest Products Journal, vol XII, n°6, June, 287-294.

555 McKenzie, W., Karpovich, H. (1975) Wear and blunting of the tool corner in cutting a wood-  
556 based material Wood Sci. Technol., (9), 1, 59-73

557 McKenzie, W.M., Ko, P., Cvitkovic, R., Ringler, M. (2001) Towards a model predicting  
558 cutting forces and surface quality in routing layered boards. Wood Sci. Technol. 35 : 563-569

559 Marchal, R. (1989) Valorisation par tranchage et déroulage des bois de chênes  
560 méditerranéens. INPL PhD thesis, Nancy, November 1989, 294p.

561 Marchal, R., Dai, C., Wang, B. (2000) La surveillance du déroulage par analyse acoustique et  
562 vibratoire : Résultats préliminaires, 6ème Séminaire PPF "Maîtrise globale du procédé  
563 d'enlèvement de matière et des techniques associées" – ENSAM Metz, 12 p.

564 Marchal, R., Jullien, D., Mothe, F., Thibaut, B. (1993) Mechanical aspects of heating wood  
565 in rotary veneer cutting. Proceeding of IWMS 11, May, 25-27 1993, 257-278

566 Marchal, R., Negri, M. (1997) Rotary cutting of high density wood: lathe-settings  
567 programmed variation to improve the transient phases crossing. Proceeding of IWMS 13,  
568 June 17-20, 1997, 547-559

569 Merchant M.E.(1945) Mechanics of the metal cutting process (I) – orthogonal cutting and a  
570 type II chip, J. Appl. Phys.16 (1945) 267–275.

571 Mothe, F. (1988) Aptitude au déroulage du bois de Douglas. Conséquences de l'hétérogénéité  
572 du bois sur la qualité des placages. INPL PhD thesis, Nancy, October 1988, 173p.

573 Mothe, F., Marchal, R. (2001) Influence of the nosebar settings on tool instabilities in the  
574 peeling process. Proceedings of the 15th International Wood Machining Seminar, Los  
575 Angeles, July 30-August 1, 2001, 309-329



576 Mothe, F., Thibaut, B., Marchal, R., Negri, M. (1997) Rotary cutting simulation of  
577 heterogeneous wood : application to douglas fir peeling. Proceedings of the 13th International  
578 Wood Machining Seminar, Vancouver, June 17-20, 1997, 411-428.

579 Movassaghi, E. (1985) Influence des paramètres microdensitométriques du bois sur les efforts  
580 de coupe et la qualité des placages de Douglas et de Châtaignier obtenus par déroulage. Thèse  
581 Docteur Ingénieur, INPL Nancy 1985.

582 Murase, Y., Harada, S. (1995), Acoustic Emission Characteristics in Wood Cutting I : Effect  
583 of the grain angles on the amplitude of the acoustic emission, Mokuzai Gakkaishi 41(4):373-  
584 379.

585 Murase, Y., Nogami, H., Ohuchi, T., (2004) Acoustic Emission Characteristics in Veneer  
586 with a Roller Bar, Proceedings of the 2nd ISWM, Vienna, Austria, 5–7th Jul., pp. 185-189.

587 Nagatomi, K., Yoshida, K., Banshoya K., Murase, Y., (1993) Recognition of wood cutting  
588 conditions through cutting sounds I: Effect of tool system's stiffness and tool wear on the  
589 generation of sound in cutting parallel to the grain, Mokuzai Gakkaishi 39 (5):521-528.

590 Nagatomi, K., Yoshida, K., Banshoya K., Murase, Y. (1999) Relation between veneer quality  
591 and peeling sound in the peeling of sugi, 14th IWMS, France, Sept., pp. 681-690.

592 Oxley, P.L.B. (1989) Mechanics of machining An analytical approach to assessing  
593 machinability. Chichester : Ellis horwood Limited publishers, 1989, 242 p.

594 Palmqvist, J., (2003) Parallel and normal cutting forces in peripheral milling of wood. Holz  
595 Roh Werkst (2003) 61 (6): 409-415

596 Palmqvist, J., Johansson, G. (1999) Cutting forces in peripheral milling of wood. Proceeding  
597 of IWMS 14, September 12-19, 1999, 751-760

598 Scholtz, F., Troeger, J. (2005) Modelling of cutting forces. Proceeding of IWMS 17,  
599 September 26-28, 2005, 260-271

600 Sinn, G., Beer, Gindl, M., Parsh, R., Kisselbach, A., Standler, F., Stanz-Tschegg, S. (2005)  
601 Analysis of cutting forces in circumferential flat milling of MDF and particleboard.  
602 Proceeding of IWMS 17, September 26-28, 2005, 80-87

603 Sinn, G., Mayer, H., Zettl, B., Ede, C., Beer, P. (2004) Application of ultrasonic-assisted  
604 cutting in wood machining. Proceedings of 2<sup>nd</sup> International symposium on wood machining,  
605 Vienna, Austria, July 5-7, 2004, 499-503

606 Stewart, H.A. (1977) Optimal rake angle related to selected strength properties of wood.  
607 Forest Products Journal, 27(1), 51-53

608 Stewart, H.A. (1991) A comparison of tool materials, coatings, and treatments related to tool  
609 wear during wood machining. Forest Products Journal. 41(9): 61-64

610 Tanaka, C., Cyra, G., Nakao, T., Yoshinobu, M., Katayama, H. (1997) On-line Control of  
611 Feed-Speed in Routing, Mokuzai Gakkaishi 43 (7): 544-550.

612 Thibaut, B. (1988) Le processus de coupe du bois par déroulage. Habilitation Thesis,  
613 Université des Sciences et Techniques du Languedoc, Montpellier, 354p.

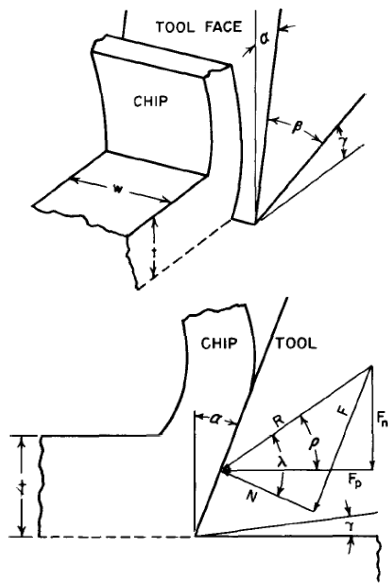
614 Thibaut, B. (1995) Basic process in veneer cutting. Summary of main experimental results  
615 and proposed simplistics models. Conférence invitée, Séminaire du National Industrial  
616 Research Institute of Nagoya, Japon, 26 juin 1995, 19 p+vidéo.

617 Thibaut, B., Beauchêne, J. (2004) Links between wood machining phenomena and wood  
618 mechanical properties: the case of 0°/90° orthogonal cutting of green wood. Proceedings of  
619 2<sup>nd</sup> International symposium on wood machining, Vienna, Austria, July 5-7, 2004, 149-160

620 Timoshenko, S. P., Goodier, N. (1951) Theory of Elasticity. McGraw-Hill, New York.  
621 International Student Edition, 506 p

622 Vazquez-Cooz, I., Meyer, R.W. (2006) Cutting forces for tension and normal wood of maple.  
623 Forest Products Journal 56 (4): 26-34

624 Woodson, G.E., Koch, P. (1970) Tool forces and chip formation in orthogonal cutting of  
625 loblolly pine. Forest Service Research Paper SO-52. U.S. Department of Agriculture  
626



- $\alpha$  – Rake angle: angle between the tool face and a plane perpendicular to the direction of tool travel.
- $\beta$  – Sharpness angle: angle between the tool face and back.
- $\gamma$  – Clearance angle: angle between the back of the tool and the work surface behind the tool.
- $t$  – Thickness of chip before removal from the workpiece.
- $w$  – Width of undeformed chip.
- $F_n$  – Normal tool force: force component acting perpendicular to parallel tool force and perpendicular to the surface generated.
- $F_p$  – Parallel tool force: force component acting parallel to tool motion in workpiece, i.e., parallel to cut surface.
- $R$  – Resultant tool force: the resultant of normal and parallel tool force components.
- $P$  – Angle of tool force resultant: the angle whose tangent is equal to the normal tool force divided by the parallel tool force.
- $F$  – Friction force: force component acting along the interface between tool and chip.
- $N$  – Normal to the friction force: force component acting normal to tool face.
- $\lambda$  – Angle between resultant tool force and the normal frictional force; the angle whose tangent is equal to the friction force divided by the normal friction force.

Figure 1 Orthogonal decomposition of the cutting force (in Woodson and Koch, 1970)

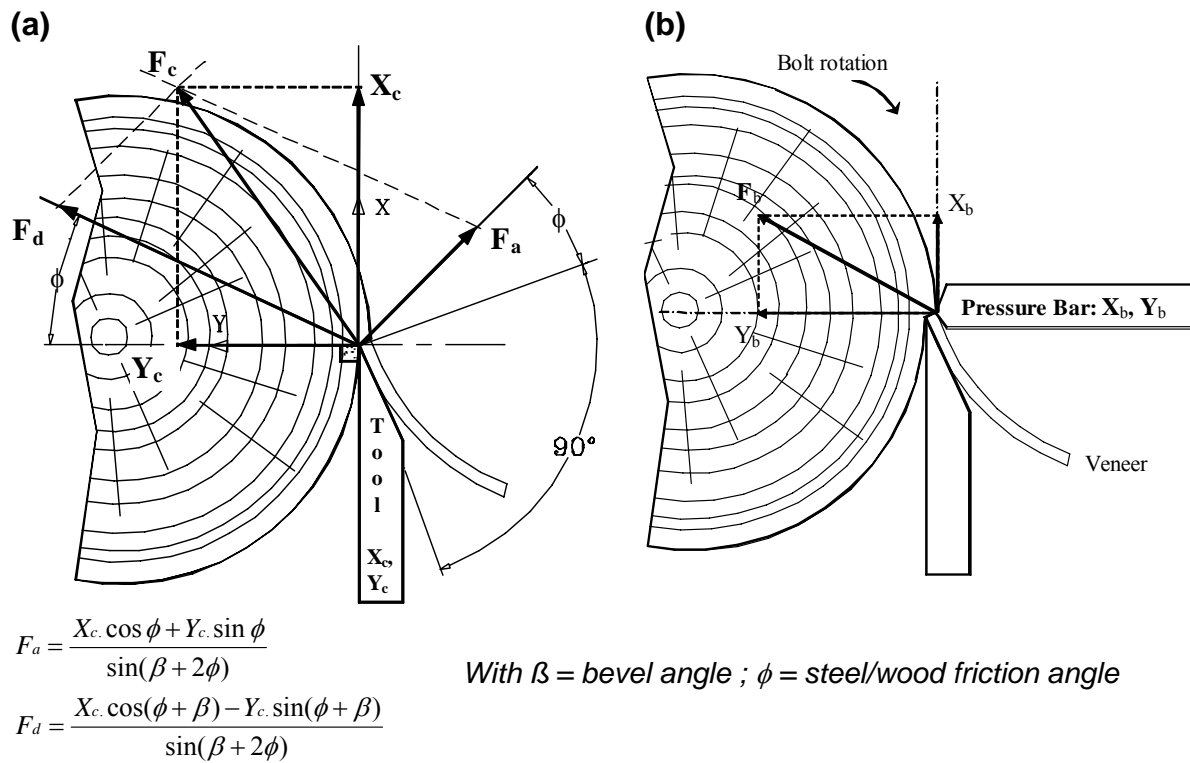


Figure 2: Cutting and pressure bar forces in peeling processes. (a) orthogonal and facial components of the resultant cutting forces  $F_c$  (b) orthogonal components of the resultant pressure force  $F_b$  (in Butaud et al 1995)

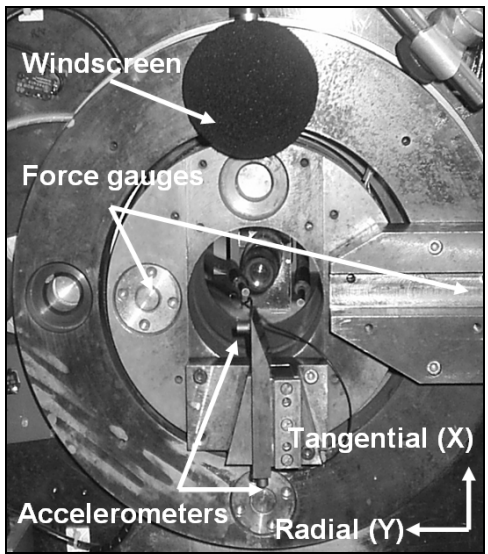
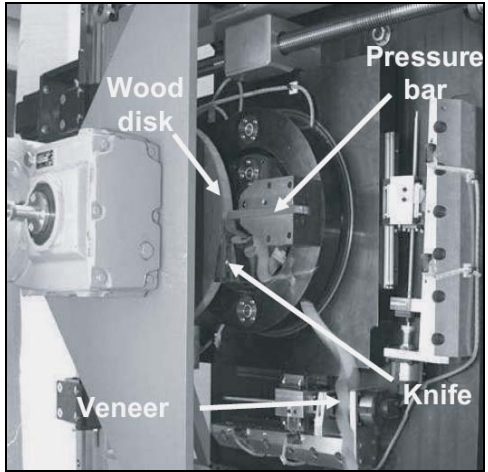


Figure 3 The instrumented microlathe in ENSAM

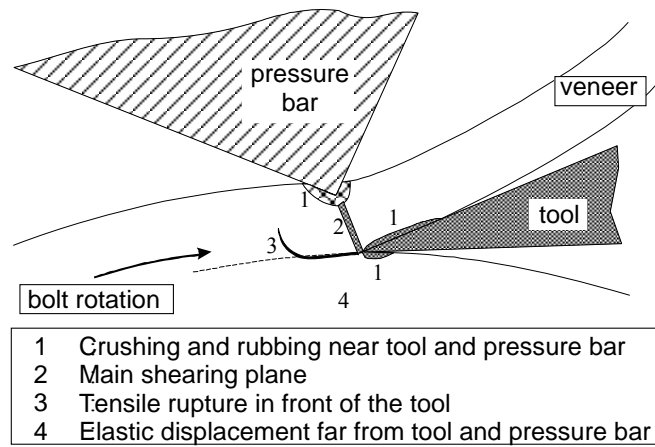


Figure 4 Basic processes in veneer cutting (in Beauchêne 1996)

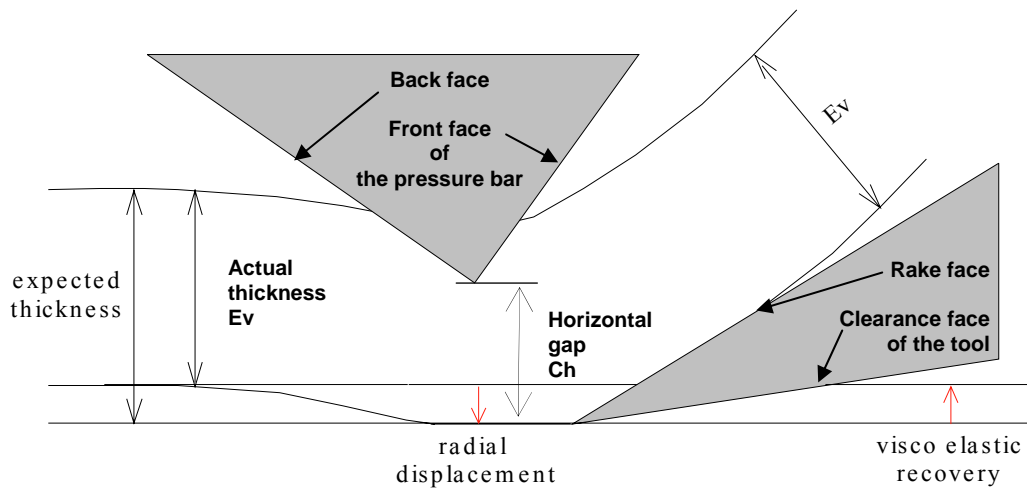
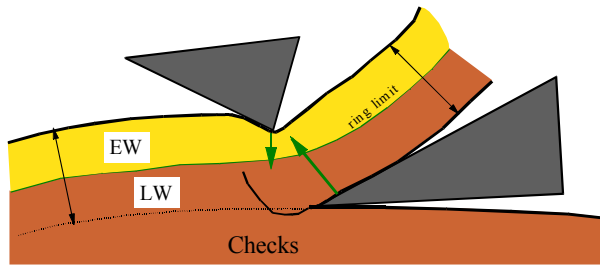


Figure 5 Consequence of the radial displacement of wood on veneer thickness at the tip level due to the cutting forces.



(a)



(b)

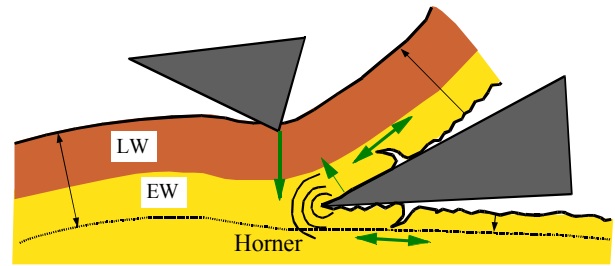


Figure 6 Specific problems encountered with heterogeneous species. (a) Ring limit crossing the veneer: the high density near the tool increases the risk of lath checks since the low density near the pressure bar prevents it to counteract. (b) Early wood/late wood transition: the soft wood around the tool is crushed at the tool tip and torn by the friction on the tool faces; the bar force is increased by dense wood and tends to reduce the veneer thickness by moving the cutting plane above the tool.

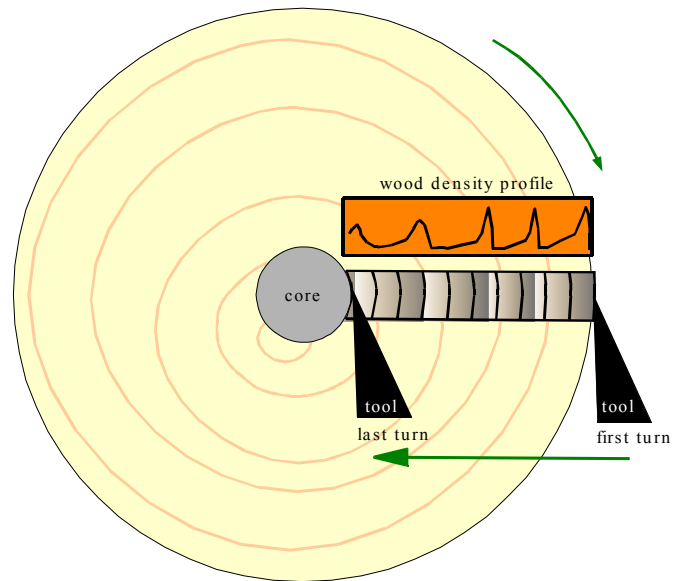


Figure 7 Work of the peeling simulator. The forces and wood displacements are computed at each turn at the same radial position. The wood density profile is the basis for predicting the mechanical properties along the radius.

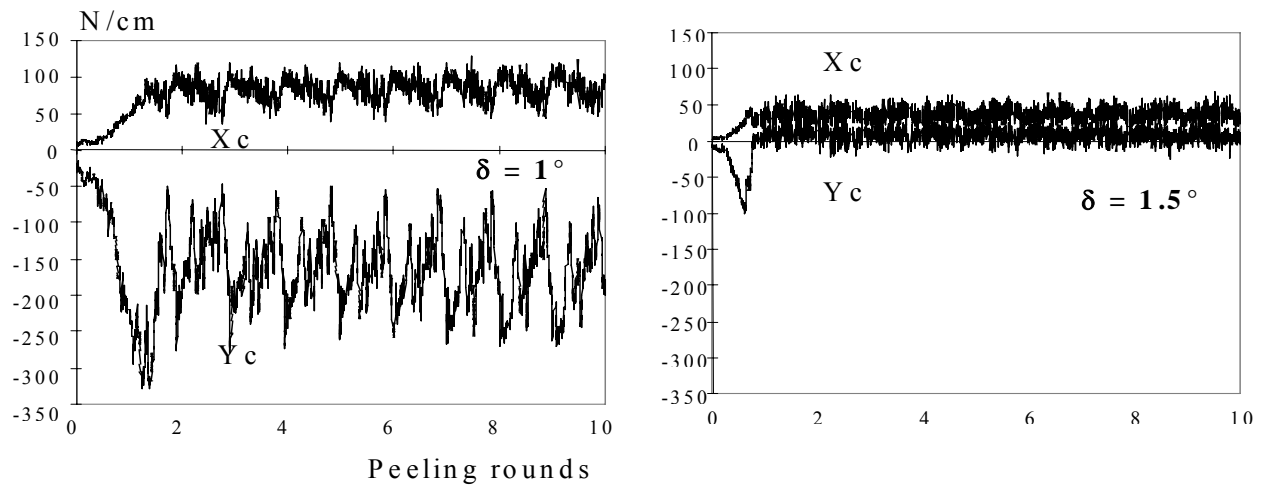


Figure 8 Experimentally obtained diagrams. Influence of the clearance angle  $\delta$  on the orthogonal cutting forces distribution (Marchal and Negri 1997) in the case of peeling thin veneers (evergreen oak; nominal thickness = 0.6 mm; cutting speed = 2 mm/s)

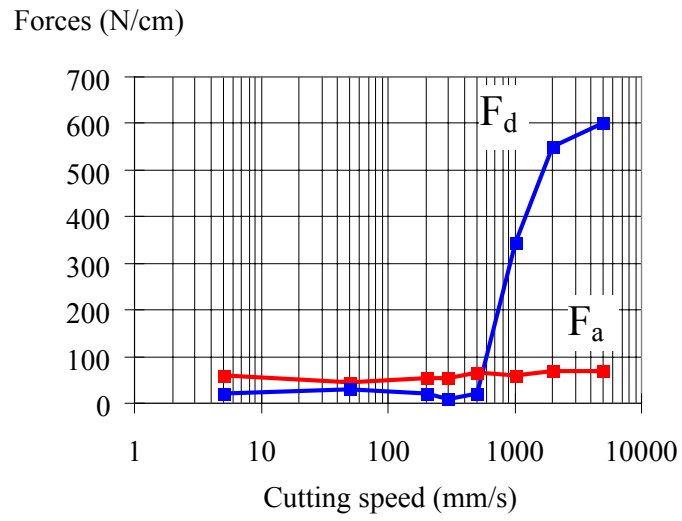


Figure 9 Evolution of the two facial components of the resultant cutting force with the cutting speed (Decès-Petit 1996). (Walnut; nominal thickness = 1 mm; clearance angle = 0°)

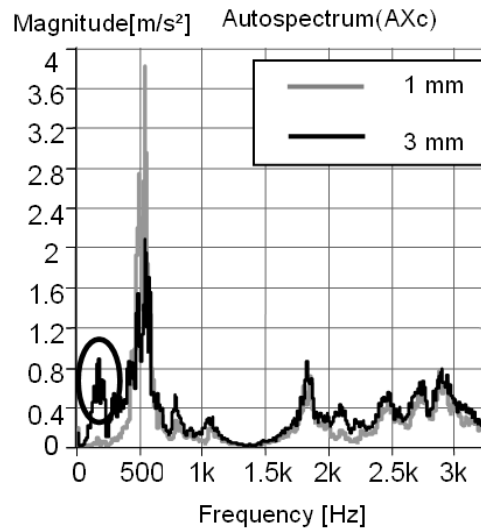


Figure 10 Lathe check signature (spectrum from knife accelerometer in tangential direction (AX<sub>c</sub>). The signature (circled) is mainly visible for the higher thickness, only very small lathe check occurring when peeling in 1 mm (grey line). Poplar, without the pressure bar, V<sub>c</sub> = 0.5m/s, well honed tool, clearance angle null, thickness of 1 mm: soft-checked veneer / thickness of 3 mm: hard-checked veneer)

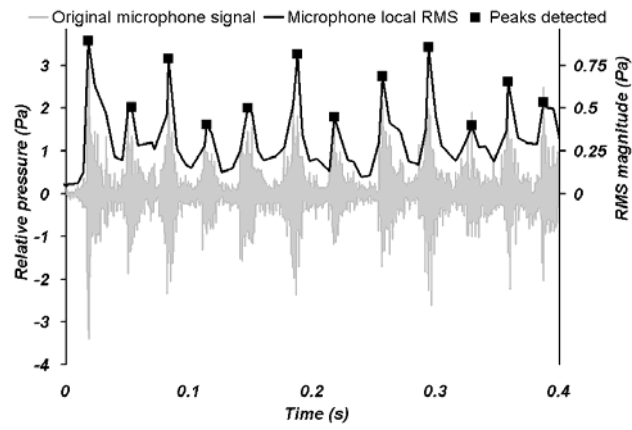


Figure 11: Original, preset, and peak detected from the microphone signal for a 3 mm thick beech veneer (Denaud et al 2007 a)

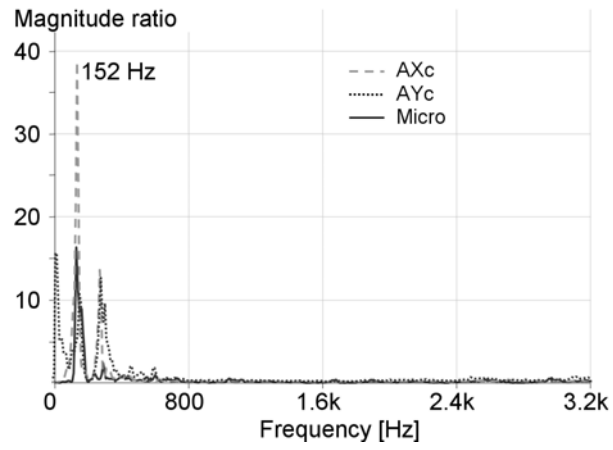


Figure 12 PSD ratio for microphone,  $AX_c$  and  $AY_c$  accelerometers (respectively in the tangential and radial direction) between 3 mm. Poplar veneer without pressure bar and reference signal.